Bis(pyrrolecarboxamide) Linked to Intercalating Chromophore Oxazolopyridocarbazole (OPC): Selective Binding to DNA and Polynucleotides

Frédéric Subra, Sandrine Carteau, Jeanne Pager, Jacques Paoletti, Claude Paoletti, and Christian Auclair*
Laboratoire de Biochimie-Enzymologie, INSERM U140, CNRS LA 147, Institut Gustave Roussy, Villejuif, France
Driss Mrani, Gilles Gosselin, and Jean Louis Imbach
Laboratoire de Chimie Bioorganique, Université des Sciences et Techniques du Languedoc, Montpellier, France
Received June 26, 1990; Revised Manuscript Received October 3, 1990

ABSTRACT: We have investigated some properties related to interaction with DNA and recognition of AT-rich sequences of netropsin–oxazolopyridocarbazole (Net–OPC) (Mrani et al., 1990), which is a hybrid groove-binder–intercalator. The hybrid molecule Net–OPC binds to poly[d(A-T)] at two different sites with K_{app} values close to 7×10^6 and 6×10^8 M^{-1} (100 mM NaCl, pH 7.0). Data obtained from melting experiments are in agreement with these values and indicate that Net–OPC displays a higher binding constant to poly[d(A-T)] than does netropsin. On the basis of viscometric and energy transfer data, the binding of Net–OPC to poly[d(A-T)] is suggested to involve both intercalation and external binding of the OPC chromophore. In contrast, on poly[d(G-C)], Net–OPC binds to a single type of site composed of two base pairs in which the OPC chromophore appears to be mainly intercalated. The binding constant of Net–OPC to poly[d(G-C)] was found to be about 350-fold lower than that of the high-affinity binding site in poly[d(A-T)]. As evidenced by footprinting data, Net–OPC selectivity recognizes TTAA and CTT sequences and strongly protects the 10-bp AT-rich DNA region 3′-TTAAGAACTT-5′ containing the *Eco*RI site. The binding of Net–OPC to this sequence results in a strong and selective inhibition of the activity of the restriction endonuclease *Eco*RI on the plasmid pBR322 as substrate. The extent of inhibition of the rate constant of the first strand break catalyzed by the enzyme is about 100-fold higher than the one observed in the presence of netropsin under similar experimental conditions.

The artificial regulation of gene expression requires the design of molecules that selectively recognize single-stranded or double-stranded nucleic acid base sequences. This can be theoretically achieved by two families of compounds including (i) synthetic antimessenger oligodeoxynucleotides, which ensure recognition of RNA complementary sequences [see Izant et al., (1985), Green et al. (1986), and Paoletti (1988) for general reviews] and (ii) oligopeptides in the series of poly(pyrrolecarboxamides) (Wartell et al., 1974) and poly(imidazolecarboxamides) (Kopka et al., 1985a,b; Lown, 1988), which bind, respectively, to A-T- and G-C-containing sequences in the minor groove of double-stranded DNA. From a pharmacological point of view, molecules designed to interfere with the functional activity of the genome should in addition display favorable permeation through cell membranes, favorable accessibility to their presumed target and resistance toward cellular lytic enzymes such as proteases and nucleases. Accordingly, various structurally modified synthetic oligonucleotides such as methylphosphonate oligonucleotides (Miller et al., 1986) and unnatural α-deoxynucleotides (Sequin, 1974; Morvan et al., 1987) as well as antimessenger oligodeoxynucleotides covalently linked to intercalating or photoactivable chromophores (Dryer et al., 1985; Hélène et al., 1985; Toulmé et al., 1986) have been prepared, and some of them were found to significantly inhibit gene expression in cell-free systems and intact cells. In the series of oligopeptides, poly(pyrrolecarboxamides) related to netropsin and distamycin covalently linked to EDTA have been found to cleave selectively double-stranded DNA at definite sequences (Schultz et al., 1982; Taylor et al., 1984), whereas more recently, oligopeptides related to netropsin linked to the intercalating chromophores actinomycin D (Dervan, 1986) or acridine have been synthesized and found to recognize AT-rich sequences. Along this line, and in view of our pharmacological purpose, we have previously synthesized (Mrani et al., 1990) netropsin-like conjugates in which the guanidine moiety of the netropsin molecule has been replaced by a tetramethylene chain linked to the intercalating chromophore oxazolopyridocarbazole (OPC) (Auclair et al., 1984; Gouyette et al., 1985). Among the different molecules synthesized, the compound displaying an oligopeptide chain identical with that of netropsin [i.e., bis(pyrrolecarboxamide) linked to an amidine moiety] (Net–OPC) (Figure 1) exhibited a markedly high affinity for poly[d(A-T)] as measured by ethidium bromide exclusion. The present paper describes in detail the binding parameters to DNAs and polynucleotides of Net–OPC in view of the nature of the binding and selective recognition of base pair sequences.

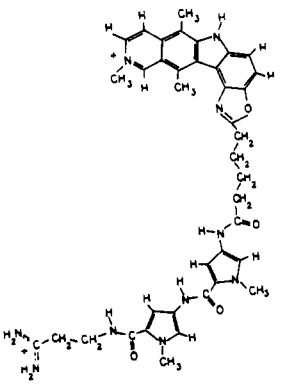

FIGURE 1: Structure of Net–OPC.

* To whom correspondence should be addressed.

0006-2960/91/0430-1642$02.50/0

Materials and Methods

Synthesis of Netropsin-OPC Conjugate. Netropsin–OPC conjugate [3-{1-methyl-4-[1-methyl-4-[4-(2-{7,10,12-trimethyl-6*H*-[1,3]oxazolo[5,4-*c*]pyrido[3,4-*g*]carbazolyl})butanecarboxamido]pyrrole-2-carboxamido]pyrrole-2-carboxamido}propionamidinediacetate] (Figure 1) (Net–OPC) has been prepared as previously described (Mrani et al., 1990). Briefly, Net–OPC was obtained from the conjugation of OPC–valerate (5-[2-(7,10,12-trimethyl-6*H*-[1,3]oxazolo[5,4-*c*]pyrido[3,4-*g*]carbazolyl)pentanoic acid (OPC–valerate) with methyl 1-methyl-4-(1-methyl-4-aminopyrrole-2-carboxamido)pyrrole-2-carboxylate. OPC–valerate is prepared from the antitumor agent 2-methyl-9-hydroxyellipticinium (Ellipticinium) (NMHE) according to a procedure previously described (Auclair et al., 1984).

DNAs and Polynucleotides. DNA from *Micrococcus lysodeikticus* (28% A+T) and *Clostridium perfringens* (69% A+T) and poly[d(A-T)] and poly[d(G-C)] were obtained from Boehringer, Mannheim (Germany) and used without further purification.

Preparation of pBR322 DNA. Escherichia coli HB101 cells transformed with the monomeric form of the plasmid pBR322 were grown to late log phase in LB medium with ampicillin (100 μg/mL) before addition of chloramphenicol (150 μg/mL). AFter continued growth at 37 °C overnight, cells were harvested by centrifugation, and the covalently closed form of the plasmid was purified by centrifugation to equilibrium in cesium chloride–ethidium bromide followed by extraction with 1-butanol saturated with TE buffer. Concentrations of DNA were evaluated from UV absorption at 260 nm.

Fluorescence Experiments. Fluorescence spectra were recorded on a SFM 23/B spectrofluorometer (Kontron, Zürich, Switzerland) equipped with a thermostated cell holder. In all cases, fluorescence experiments were performed in quartz cells (1-cm path length) thermostated at 25 °C. Scattering of excitation radiation was removed by using the appropriate emission filter.

Energy Transfer. The occurrence of energy transfer from nucleic acids to the bound drug was determined according to Weil and Calvin (1963). The relative quantum yield ratio of the bound drug upon excitation in the UV region versus excitation in the visible region was determined by using

$$\frac{Q_\lambda}{Q_{vis}} = \left(\frac{I_\lambda}{I_{vis}}\frac{E_{vis}}{E_\lambda}\right)_{bound}\left(\frac{I_{vis}}{I_\lambda}\frac{E_\lambda}{E_{vis}}\right)_{free}$$

where I and E are, respectively, the fluorescence intensity and the molar extinction coefficient at wavelengths vis = 315 nm and λ = 260–315 nm.

Viscometric Experiments. Viscometric measurements were performed at 25 °C in a semimicrodilution capillary viscometer linked to a IBM XT computer. The capacity of tested compounds to increase the length of sonicated DNAs from calf thymus, from *M. lysodeikticus*, and from *C. perfringens* was measured under standard operating conditions essentially as described by Saucier et al. (1971).

UV Melting Curves. Absorbance versus temperature profiles for DNA and drug-bound DNA duplex were determined by using a thermoelectrically controlled Uvikon spectrophotometer. Samples in 10 mM cacodylate buffer (pH 7.0) containing 10 mM NaCl were heated at a rate of 1 °C/min while both temperature and absorbance (at 260 nm) were recorded. Best fits of the melting curves dA/dT were obtained by computed nonlinear regression describing a sigmoidal equation. The melting temperatures were estimated from the corresponding first derivative of the fitted curve.

Footprinting Experiments: (*i*) *Hydroxyl Radical Footprinting.* We prepared end-labeled 220-bp restriction fragments of pBR-322 by digesting pBR322 with *Hin*dIII, labeling the ends with radioactive phosphorus, digesting with *Ssp*I, and purifying the labeled 220-bp fragment by electrophoresis on a 5% acrylamide gel and electroelution. We labeled the 3′ end by allowing the fragment to react with the Klenow fragment of DNA polymerase I along with [α-^{32}P]dATP. End-labeled DNA was added to a buffer consisting of 10 mM Tris-HCl. The volume of reaction mixture at this point was 60 μL. A 10-μL aliquot of a solution of Net–OPC dissolved in distilled water at the appropriate concentration was added to the final reaction mixture and incubated at room temperature. A stock solution of iron(II)–EDTA was prepared immediately before use by mixing equal volumes of freshly prepared 0.2 mM Fe(II) [by dissolution of $(NH_4)_2Fe(SO_4)_2{\cdot}6H_2O$] and 0.4 mM EDTA solution (10 μL), 0.3% hydrogen peroxide (10 μL), and 10 mM sodium ascorbate (10 μL) on the inner wall of a 1.5-mL Eppendorf tube containing the Net–OPC/DNA solution. The reaction was allowed to run for 2 min and then quenched by addition of 0.1 M thiourea (10 μL), 0.1 M EDTA (32 μL), 3 M sodium acetate (14 μL), and ethanol (450 μL). The DNA was precipitated at −20 °C, isolated by centrifugation, washed with cold 70% ethanol, dried using a Speed-Vac concentrator, and dissolved in formamide containing 0.1% bromophenol blue.

(*ii*) *Gel Electrophoresis.* DNA fragments were separated by electrophoresis in a gel composed of 8% polyacrylamide containing 7 M urea and Tris/borate/EDTA buffer. After 2 h of electrophoresis at 1500 V, the gels were soaked in 10% acetic acid for 10 min, dried at room temperature, and subjected to autoradiography.

(*iii*) *Densitometry.* Autoradiographs from the hydroxyl radical footprinting experiments were analyzed with a Joyce scanning microdensitometer to produce profiles from which the relative intensity of each band was measured. These intensities were calculated in terms of fractional cleavage $f = A_i/A_t$, where A_i is the area under band i and A_t is the mean of the sum of the areas under all bands in the corresponding gel lane. Protection or enhancement in the presence of drug was expressed as percent fractional cleavage compared to control.

Restriction Endonuclease Assay. Activity of the restriction endonucleases *Eco*RI and *Nru*I has been measured at 37 °C by using as substrate covalently closed pBR322 DNA, which contains a single site of breakage for both enzymes. Enzymatic activity in the absence and in the presence of drugs has been estimated by measuring the pseudo-first-order rate constants corresponding to the first (k_1) and to the second (k_2) DNA break under the following operating conditions: For *Eco*RI measurements, the experiments have been performed in a medium composed of 50 mM Tris-HCl (pH 7.5), 100 mM NaCl, 10 mM $MgCl_2$, and 1 mM DTE. For *Nru*I measurement, the medium was composed of 10 mM Tris-HCl, 100 mM NaCl, 5 mM $MgCl_2$, and 1 mM β-mercaptoethanol. Drugs to be tested and DNA (3 μg) were added to the standard incubation mixture (final volume 30 μL) 20 min before the enzyme addition. In all experiments, the concentration of enzyme was 2 units/μg of DNA. Samples (3 μL) were removed from the reaction mixture at timed intervals and immediately mixed with 17 μL of stop solution composed of 0.25 M EDTA, pH 8.0, 0.01% bromophenol blue, and 25% (w/v) sucrose. The cleavage products were separated by electrophoresis in a 1% agarose gel with a field strength of 6–8 V/cm and TBE buffer (pH 7.4) composed of 70 mM Tris,

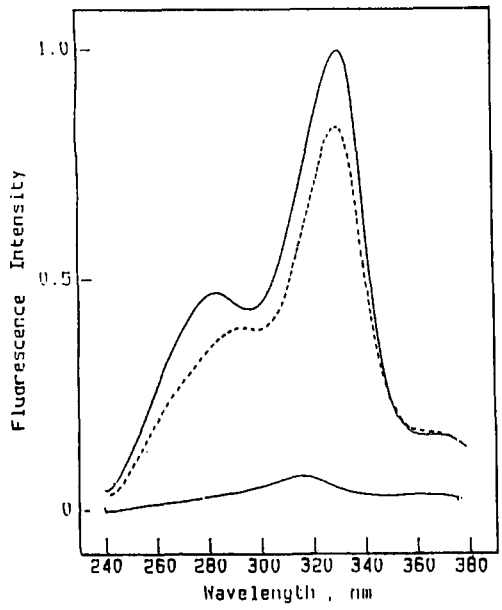

FIGURE 2: Modification of fluorescence parameters of Net–OPC upon binding to poly[d(A-T)] and poly[d(G-C)]. Uncorrected fluorescence excitation spectra of Net–OPC free in solution (lower spectrum) and in the presence of poly[d(G-C)] (middle spectrum) and poly[d(A-T)] (upper spectrum) are shown. In all experiments, the assay medium was composed of 10 mM cacodylate buffer (pH 7.0) containing 10 mM NaCl and 2 μM Net–OPC. When present, polynucleotide concentration expressed in phosphate was 90 μM (phosphate/drug = 45).

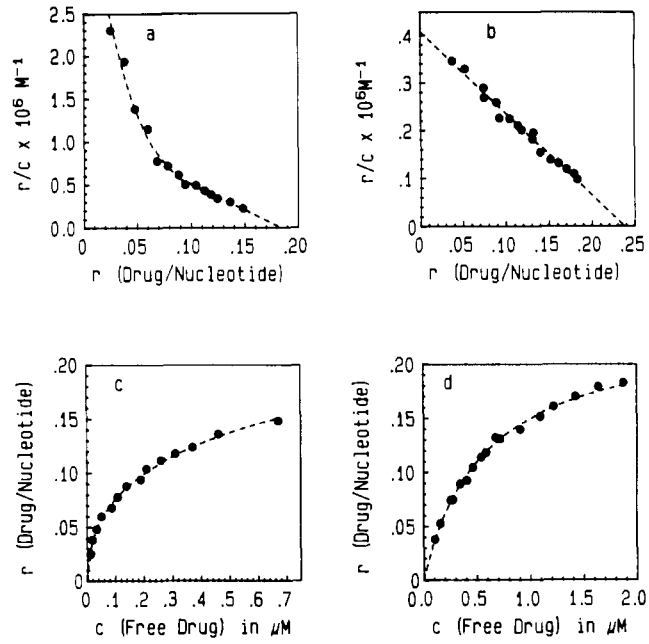

FIGURE 3: Binding curves of Net–OPC to poly[d(A-T)] (panels a and c) and poly[d(G-C)] (panels b and d). In (a) and (b), the binding curves are represented according to Scatchard. In (c) the binding curve is represented as a double-rectangular hyperbola and in (d) as a simple rectangular hyperbola. In (c) and (d), the dotted lines are the best fits to data points obtained through a nonlinear regression procedure. In all experiments, the assay medium was composed of cacodylate buffer (pH 7.0) containing either 500 mM NaCl (a) or 10 mM NaCl (b). Polynucleotide concentrations were 5.5 μM. The amount of drug bound was estimated from the fluorescence increment (ΔIF) upon drug binding by using eq 1.

2.5 mM EDTA, and 50 mM boric acid. After an overnight run, the gels were then stained under gentle shaking for 30 min in ethidium bromide solution (500 μg/L) and photographed for 1 min under 354-nm UV light on Polaroid 665 positive/negative film. For quantitative evaluation, the negatives were scanned with a gel scanner. The relative amounts of supercoiled, open circular, and linear DNA in each sample were normalized to the total DNA concentration.

Nonlinear Regression Fitting. Curves were fitted to data points using programs involving the method of Marquardt. Goodness of fit was quantitated by the least square procedure using as parameter the distance of each point from the curve. Software used included STATGRAPHICS (Statistical Graphic Corp.) and GraphPAD (ISI Software) as well as programs developed in the laboratory. Goodness of fit was assessed by the r^2 value, which is always taken higher than 0.98, and it was verified that the residuals were randomly distributed with respect to X values.

RESULTS

Fluorescence Changes of OPC Chromophore upon Binding to Polynucleotides. Binding of Net–OPC to double-stranded polynucleotides results in a strong increase in the fluorescence intensity of the OPC chromophore associated with a shift of the excitation spectrum toward longer wavelengths (Figure 2). These spectral changes are related to the binding of the chromophore to hydrophobic regions inside helical DNA (Le Pecq & Paoletti, 1967). Figure 2 shows the fluorescence uncorrected excitation spectra of free Net–OPC (recorded in the absence of DNA) and Net–OPC bound to poly[d(A-T)] or poly[d(G-C)]. The maximum excitation wavelengths are observed at 310 nm in the absence of polynucleotide (free drug) and at 330 nm in the presence of saturating concentrations of either poly[d(A-T)] or poly[d(G-C)] (bound drug). A shoulder appearing in both spectra of bound drug in the 260-nm region reflects the presence of energy transfer occurring from DNA bases to the bound chromophore; it will be described later. The fluorescence increment at the maximum excitation wavelength (V) resulting from drug binding at a saturating concentration of nucleotides can be estimated from the linear plot $1/V - 1 = f(1/[\text{nucleotide}])$. In the experimental conditions used in recording the spectra (cacodylate buffer, pH 7.0, with 10 mM NaCl), V values at 330 nm were found to be 39.4 and 29.9 upon binding of Net–OPC to poly[d(A-T)] and poly[d(G-C)], respectively.

Association Constants to Polynucleotides. The fluorescence increase of the OPC chromophore upon binding to DNA or polynucleotides allows the estimation of the amount of bound drug at the equilibrium:

$$D_b = \Delta IF/k(V - 1) \quad (1)$$

where ΔIF is the difference between the fluorescence of drug in the presence and in the absence of DNA, V is the fluorescence increment resulting from the binding to DNA estimated as indicated in Figure 2, and k is the factor that relates the concentration of free drug to the fluorescence intensity of the solution. Binding curves so obtained can be plotted according to Scatchard, leading to the estimation of the association constant values (K_{app}) and the maximum amount of drug bound per nucleotide at saturating concentration (r_{max}), which in turn allows the estimation of the apparent size (n) of the binding site. Typical Scatchard plots describing the binding of Net–OPC to poly[d(A-T)] and poly[d(G-C)] are shown in Figure 3, panels a and b. The Scatchard plot in Figure 3a shows that the binding of Net–OPC to poly[d(A-T)] occurs at two different sites. The curve corresponds to

$$r/c = K_1(n_1 - r_1) + K_2(n_2 - r_2) \quad (2)$$

where $r = r_1 + r_2$, r_1 and r_2 are the amount of drug bound per nucleotide to site 1 and to site 2, respectively, n_1 and n_2 are

Table I: Variation of the Association Constant K_{app} of Net–OPC for Poly[d(A-T)] and Poly[d(G-C)] as a Function of the Salt Concentration

NaCl concn (mM)	K_{app} ($\times 10^6$ M^{-1})		
		poly[d(A-T)]	
	poly[d(G-C)]	site 1	site 2
10	7.20	27000.0[a]	61.0[a]
20	4.94		
50	2.76		
100	1.72	600.0[a]	7.1[a]
150	1.30		
300		96.9	2.39
500		50.0	1.90
750		22.5	1.07
1000		13.8	0.82
slope[b]	−0.64 ± 0.01	−1.62 ± 0.09	−0.92 ± 0.14

[a] Indicates extrapolated values calculated by using eq 5. [b] Slope of the straight line obtained from the linear regression of eq 5 such as log K_{app}/log $[Na^+] = -Z\psi$.

the number of sites 1 and 2 per nucleotide, and c is the concentration of drug free in solution. This binding process is also described by a double-rectangular hyperbola (Figure 3c):

$$r = \frac{n_1}{K_{d1}/c + 1} + \frac{n_2}{K_{d2}/c + 1} \quad (3)$$

where K_{d_1} and K_{d_2} are the dissociation constants of the drug to sites 1 and 2.

The nonlinear regression of eq 3 by the Marquardt algorithm allows the estimation of the values of the apparent association constant K_{app} ($1/K_d$) for both binding sites as well as n_1 and n_2. K_{app} values obtained from the best fit to data points of the plot shown in Figure 3c were the following: $K_1 = 5.0 \times 10^7$ M^{-1}, $K_2 = 1.7 \times 10^6$ M^{-1}, $n_1 = 0.062$, and $n_2 = 0.17$. In contrast to the above data, the binding of Net–OPC to poly[d(G-C)] as plotted according to Scatchard is described by a straight line, suggesting the occurrence of a single type of binding sites (Figure 3b). Accordingly, the binding curve is well described by a simple rectangular hyperbola:

$$r = \frac{n}{K_d/c + 1} \quad (4)$$

The best fit to data points of the curve shown in Figure 3d yields an n value of 0.23, which is consistent with an apparent binding site size of roughly two base pairs as expected for a monointercalating agent and a K_{app} value of 1.72×10^6 M^{-1}. It should be noticed that, because of the markedly high affinity of Net–OPC for poly[d(A-T)], high salt concentrations (up to 300 mM) are required to establish the binding curves. In the usual operating conditions (100 mM NaCl), the equilibrium conditions are not reached and the binding occurs in a stoichiometric manner. In order to compare the association constant values of Net–OPC for poly[d(A-T)] and poly[d(G-C)] under identical experimental conditions, we have determined the different K_{app} values obtained at different salt concentrations. According to Record et al. (1976), the dependence of K_{app} on ionic strength is described by

$$\text{d log } K_{app}/\text{d log } [Na^+] = -Z\psi \quad (5)$$

where Z is the charge involved in the binding and ψ is the fraction of counterions associated with each DNA phosphate (for double-stranded DNA, $\psi = 0.88$). The plot of log K_{app} versus log $[Na^+]$ corresponding to eq 4 yields straight lines whose slopes (-0.88 Z) correspond, therefore, to the number of charges involved in the binding process. Table I shows the variation of the K_{app} of Net–OPC for the two bindings sites in poly[d(A-T)] and for the single binding site in poly[d(G-C)]

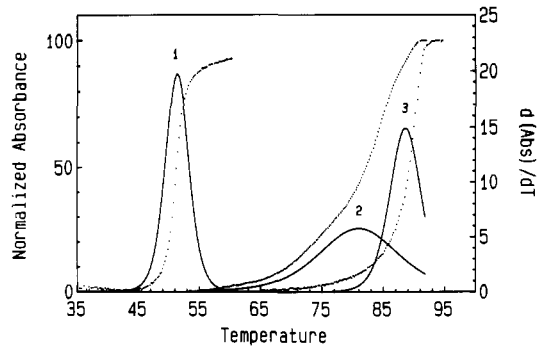

FIGURE 4: Melting curves of poly[d(A-T)], recorded as indicated under Materials and Methods in the absence (curve 1) or in the presence of either netropsin (curve 2) or Net–OPC (curve 3). Solid curves represent the first derivative of the best fit of the melting curves as described by eq 6. The assay medium was composed of cacodylate buffer (pH 7.0) containing 10 mM NaCl and 60 μM poly[d(A-T)].

as a function of the salt concentration. It appears clear that, in poly [d(A-T)], the binding to the site of higher affinity involves the two positive charges present on the molecule, whereas the binding to the site of lower affinity involves only one positive charge. In poly[d(G-C)], the binding to the single site involves one positive charge. By using the slope values of the different straight lines described by eq 4, K_{app} for poly[d(A-T)] corresponding to lower salt concentrations can be extrapolated. For 100 mM NaCl, the extrapolated value of K_{app} of Net–OPC for the first site in poly[d(A-T)] appears to be markedly high compared to the K_{app} for poly[d(G-C)] (ratio = 349). This is consistent with the selective binding of the bis(pyrrolecarboxamide) moiety to A-T-containing sequences. The extrapolated K_{app} for the second binding site appears to be 84-fold lower and therefore appears to be of the same order of magnitude as the K_{app} for poly[d(G-C)].

Melting Experiments. This set of experiments has been performed in order to compare the DNA binding parameters of Net–OPC and netropsin under similar experimental conditions. We have first of all investigated the effect of Net–OPC on the melting transition of poly[d(A-T)]. In the absence of drug, poly[d(A-T)] undergoes a sharp melting transition occurring at 51 °C (Figure 4, curve 1). The melting curve so obtained is satisfactory described by

$$A = \frac{A_{max}}{(T_m/T)^{n_H} + 1} + B \quad (6)$$

in which A is the absorbance of the DNA at 260 nm, A_{max} is the plateau of the curve, T is the temperature, n_H is a coefficient (Hill coefficient) that reflects the cooperative index of the melting process, B is the absorbance of the DNA when $T \rightarrow 0$ ($B = 0$ when the relative absorbance is used, as in Figure 4), and finally T_m is the melting point of the DNA (the temperature where $A = A_{max}/2$). Nonlinear regression fitting of the data points allows the accurate determination of T_m and n_H, and the curve so estimated can be represented as the first derivative (Figure 4). Using this procedure, we find that the melting of poly[d(A-T)] is adequately described when $n_H = 0.35$, which corresponds to a high positive cooperative effect due to the homogeneous sequence of the polynucleotide. The addition of saturating concentrations of Net–OPC was found to strongly raise the melting temperature of poly[d(A-T)] (curve 2 in Figure 4), indicating, as expected, that the drug binds to double-stranded DNA in preference to the single-stranded form. Moreover, the n_H parameter drops to 0.098 whereas the differential melting curve became very broad. This feature is consistent with the occurrence of a heterogeneous mode of binding of the drug to poly[d(A-T)] (at least

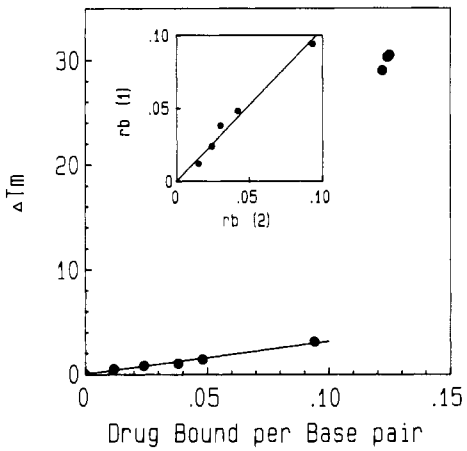

FIGURE 5: Variation of the melting temperature of poly[d(A-T)] as a function of Net–OPC bound. Conditions were as indicated in the legend to Figure 4 except that the Net–OPC concentration is a variable. The amount of drug bound to poly[d(A-T)] was calculated from the Scatchard equation by using $K_{app} = 10^{10}$ M^{-1} and a binding site size of 8 base pairs. Insert: Correlation between the amount of drug bound, calculated as indicated above [$r_b(2)$], and the amount of drug bound, calculated from eq 7 [$r_b(1)$] (see the text).

two modes of binding as indicated by the Scatchard plots). Under similar experimental conditions, the addition of netropsin results in a higher increase of the melting temperature of poly d(A-T) (curve 3 in Figure 4) whereas the n_H parameter remains high (0.29) and the differential melting curve sharp. This is in agreement with the occurrence of a single mode of binding. The effect of increasing concentrations of Net–OPC on the melting temperature of poly[d(A-T)] has been further examined, with the results indicated in Figure 5. As previously stated by Crothers (1971), the linear part of the curve (where the number of binding sites is in excess compared to the amount of drug bound) is described by

$$\frac{\Delta T_m}{r_b} = -\frac{RT_m T_m'}{\Delta H} \tag{7}$$

where r_b is the amount of drug bound per base pairs, T_m and T_m' are the melting temperature of poly[d(A-T)] in the absence and in the presence of saturating concentrations of drug, respectively, and ΔH is the enthalpy of melting of one A-T base pair.

Using a ΔH value of −7100 cal/mol (Marky & Breslauer, 1982) and a T_m' value of 81 °C yields a slope ($\Delta T_m/r_b$) of 31.2, from which can be estimated the theoretical r_b values (insert in Figure 5). These values are very close to r_b values calculated from the Scatchard equation by using a K_{app} up to 10^{10} M^{-1} and a binding site size of 8 base pairs. Both K_{app} and binding site size so estimated are in good agreement with the data provided by the plots in Figure 3, panels a and c, and with the K_{app} values calculated as shown in Table I. In the presence of saturating concentration of drug, one can consider the following (Crothers, 1971):

$$\Delta T_m = -\frac{RT_m T_m'}{\Delta H} B_h \log K_{app} \tag{8}$$

where B_h is the number of binding sites per base pair and K_{app} is the association constant value of the drug for the polynucleotide. In this occurrence, K_{app} can be calculated:

$$\log K_{app} = -\frac{\Delta T_m \Delta H}{RT_m T_m' B_h} \tag{9}$$

Calculation of K_{app} of Net–OPC to poly[d(A-T)] by using a binding site size of 8 base pairs ($B_h = 0.125$) yields a K_{app} value of 1.0×10^7 M^{-1}, which appears to be extremely low compared to the values provided by the binding curves. This discrepancy likely arises from the fact that the drug eventually binds to both helix and coil, which results in an underestimation of ΔT_m. In view of comparative investigations, we have nevertheless examined the thermal denaturation of natural DNAs and synthetic polynucleotides in the absence and in the presence of saturating concentrations of either Net–OPC or netropsin and attempted to estimate the apparent association constants (K_{app}) of these drugs by using eq 9. B_h values were taken as 0.125 (8 base pairs) and 0.2 (5 base pairs) for Net–OPC and netropsin, respectively. Results summarized in Table II show that, for all tested DNAs, the binding of Net–OPC or netropsin results in a marked increase of the melting temperature of the double helix. It should be noticed that both drugs exhibit a low ΔT_m and consequently a low binding constant to calf thymus DNA, which is in agreement with the expected selective recognition of A-T-rich sequences. Accordingly, the binding of both drugs to DNA from *C. perfringens*, which contains 69% A-T base pairs, as well as to poly[d(A-T)] and poly[d(A)·d(T)] appears to be markedly more efficient. The estimated binding constant value of Net–OPC to DNA from *Clostridium* as well as to the alternating polynucleotide poly[d(A-T)] is clearly higher than that of netropsin. Finally, both drugs display the highest binding constant to the homopolymer poly[d(A)·d(T)].

Table II: Melting Curves of Poly[d(A-T)][a]

		netropsin		Net–OPC	
DNA	T_m	T_m'	K_{app}	T_m'	K_{app}
calf thymus	73	92	5.5×10^2	81	75.0
Clostridium	65	92	8.5×10^3	83.7	3.9×10^4
poly[d(A-T)]	51	89	6.3×10^5	81	1.0×10^7
poly[d(A)·d(T)]	58	>108	$>1.0 \times 10^7$	89.7	7.0×10^7

[a] Melting experiments were performed in cacodylate buffer, pH 7.0, containing 10 mM NaCl. T_m indicates the melting temperature of the DNA measured in the absence of drug, and T_m', that measured in the presence of saturating concentrations of drug (drug/phosphate = 10). K_{app} was calculated as described in the text by using eq 8.

Viscometric Data. Information on the nature of the binding to DNA (intercalation versus external binding) can be provided by the viscometric determination of the length increase of sonicated DNA. The experiments have been performed with natural DNAs, which lead to more suitable sonicated preparations than those obtained with the synthetic nucleotides. In this technique, the theoretical treatment of the viscometric data has shown that if log η/η_0 is plotted vs log $(1 + 2r)$, where η and η_0 are the intrinsic viscosity of sonicated DNA in the presence and in the absence of the tested drug and r is the number of molecules bound per nucleotide, the slope value of the straight line so obtained is expected to be near 2.2 for monointercalating agents (Saucier et al., 1971). The slope value obtained (1.01) in the presence of DNA isolated from *C. perfringens* and containing 69% A-T base pairs suggests that OPC is partly intercalated in all binding sites or that typical intercalation occurs in about 50% of the binding sites only. Similar behavior is observed in the presence of DNA from *M. lysodeikticus* containing 72% G-C base pairs. However, the slope value of 1.47 is more consistent with typical intercalation. Accordingly, the apparent binding site size of two base pairs for Net–OPC binding to poly[d(G-C)] as determined from the Scatchard plot (Figure 3B) is as well consistent with an intercalative mode of binding. Finally, and as previously described (Auclair et al. 1988), a slope value close to 2 is obtained when the OPC molecule alone is bound to either calf thymus DNA or to DNAs from *C. perfringens* and *M. lysodeikticus*. Under similar experimental conditions, the

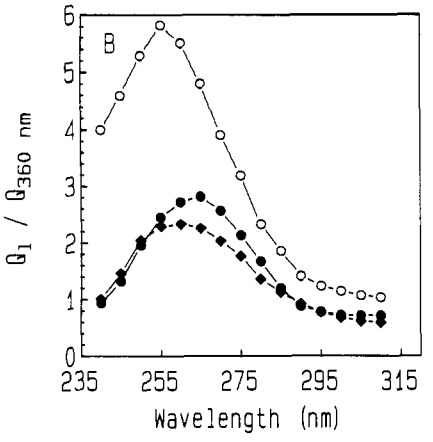

FIGURE 6: Energy transfer data related to intercalation of Net–OPC in DNAs and polynucleotides. The relative quantum yield was estimated from the absorbance and corrected fluorescence spectra of drugs bound to DNA according to Weil and Calvin (1963). The assay medium was composed of cacodylate buffer, pH 7.0, containing 100 mM NaCl. (○) OPC chromophore and calf thymus DNA; (●) Net–OPC and poly[d(G-C)]; (◆) Net–OPC and poly[d(A-T)]. In all experiments, the DNA or polynucleotide concentration was between 80 and 90 μM and the drug to nucleotide ratio was in the range of 0.04.

binding of netropsin to all tested DNAs did not result in a significant change of the viscosity.

Energy Transfer. Additional information related to the nature of the binding of the Net–OPC-containing chromophore can be obtained from energy transfer data. The occurrence of energy transfer from DNA bases to bound chromophores can be revealed by calculation of the ratio Q_λ/Q_{vis} (see Materials and Methods), which indicates the relative quantum yield of the bound drug upon excitation in the UV (Q_λ) region vs excitation in the visible region (Q_{vis}) (Weil & Calvin, 1963; Le Pecq & Paoletti, 1967). If energy transfer occurs, this ratio must be greater than unity. Energy transfer is believed to take place only with compounds in close contact with DNA bases, as it occurs for drugs intercalated into nucleic acids (Le Pecq & Paoletti, 1967; Reinhardt et al., 1982). Figure 6 shows that, in the presence of both poly[d(A-T)] and poly[d(G-C)], energy transfer from the bases to the OPC chromophore of Net–OPC occurs. However, the maximum values obtained are markedly lower than those obtained in the presence of the OPC molecule alone, which displays under similar experimental conditions maximum energy transfer of 5.7 in poly[d(A-T)], 5.3 in poly[d(G-C)], and 6.0 in calf thymus DNA (open circles in Figure 6B). The lower values obtained with Net–OPC are in agreement with the viscometric experiments and confirm that, in Net–OPC, the chromophore is partly intercalated or distributed in both intercalating sites and external binding sites. Furthermore, the higher energy transfer value observed in the presence of poly[d(G-C)] is as well in agreement with the best accommodation of the chromophore in intercalating site as suggested by both Scatchard plots and viscometric results.

Footprinting Experiment. Typical OH• radical induced cleavage patterns for the first 3′–5′ 40-mer of the 220-mer pBR322 fragment are presented in Figure 7A. The experiment performed in the presence of 10^{-8} M Net–OPC shows significant protection against cleavage essentially located at the *Eco*RI site 3′-CTTAAG-5′. In the presence of 10^{-7} M Net–OPC, four protected sites are visible, each clearly centred at CTT and CT regions. The differential cleaving plots (Figure 7, panels B and C) show that the extent of protection is markedly pronounced at the *Eco*RI site. It should be noticed that the cleavage of certain of certain bonds in the flanking

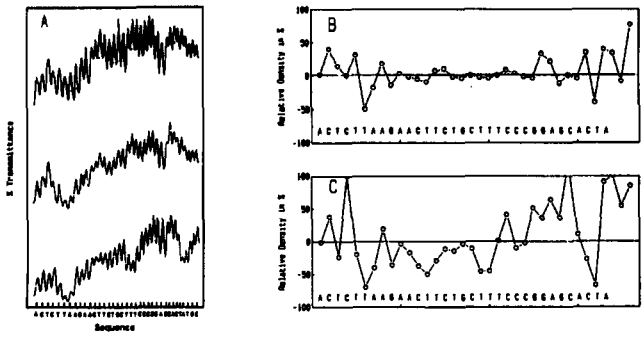

FIGURE 7: Hydroxyl radical footprinting of a *Eco*RI site containing a pBR322 DNA fragment in the presence of increasing concentrations of Net–OPC. (A) Densitometric scans of selected autoradiographic data of a 34-base-pair *Hin*dIII/*Ssp*I restriction fragment of pBR322 DNA. Upper scan, Fe–EDTA alone; middle scan, plus 10^{-8} M Net–OPC; lower scan, plus 10^{-7} M Net–OPC. (B and C) Differential cleavage plots representing (B) 10^{-8} M and (C) 10^{-7} M Net–OPC-induced difference in susceptibility of the pBR322 DNA fragment (3′ → 5′ reading left to right) to OH• radical degradation. Relative density is the measure of the fractional cleavage of any bond in the presence of drug versus the fractional cleavage of the same bond in the control for a similar extent of overall degradation. Negative values indicate protection; positive values, enhancement.

regions of the protected sites is strongly increased. This effect is especially noticeable around the cytosines. According to the X-ray crystal structure of netropsin–DNA complex (Kopka et al., 1985a), it was expected that the bis(pyrrole) moiety of Net–OPC preferentially binds to TTAA in the *Eco*RI site. In addition, from the data provided by the Scatchard plots, it could be expected to find a large protection upon Net–OPC binding corresponding to a site size of about 8–10 base pairs. That is in fact the kind of result obtained, since most bonds in the A-T-rich *Eco*RI site containing sequence 3′-TTAA-GAACTT-5′ appeared to be well protected. According to this hypothesis, CTT regions would be efficiently protected by the binding of the OPC chromophore, whereas the region of binding of the aliphatic linker (AA) appears to be less well protected.

Action on Restriction Endonucleases EcoRI and NruI. From a biological point of view, selective recognition of a given sequence by drugs should result in the selective alteration of biological functions involving similar sequence recognition. A suitable model is provided by testing the effect of drugs on the catalytic activity of restriction endonucleases that selectively produce strand breakage at a discrete site on DNA. We have therefore tested the inhibitory effect of Net–OPC and netropsin on *Eco*RI and *Nru*I, which selectively produce double-strand breaks at 5′-GAATTC and 5′-TCGCGA sequences, respectively. In the presence of supercoiled pBR322 DNA (form I) as substrate, the catalytic action of these enzymes results in a double-strand break occurring within a single cleavage site and leading to the formation of linear DNA (form III). The reaction occurs in two consecutive steps involving the production of nicked circular DNA (form II) as transient intermediate:

$$\text{form I} \xrightarrow{k_1} \text{form II} \xrightarrow{k_2} \text{form III} \qquad (10)$$

where k_1 and k_2 are the rate constants of the first and the second strand break, respectively. Forms I, II, and III can be efficiently separated by gel electrophoresis (Figure 8A), and the variation of the relative concentrations of the three forms during the time course of the enzymatic reaction can be accurately estimated. Under appropriate operating conditions, the first and the second nicking reaction occur according to pseudo-first-order kinetics (Halford & Goodall,

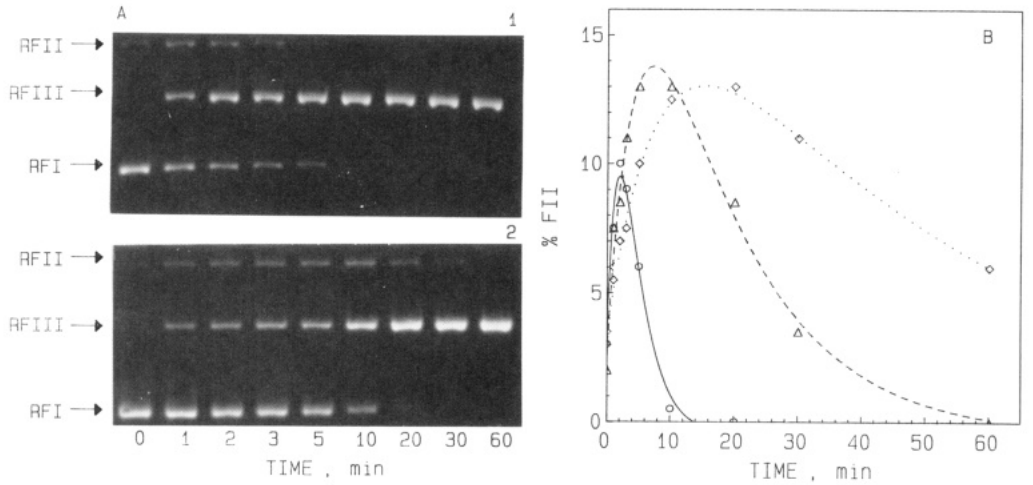

FIGURE 8: Effect of Net–OPC on the catalytic activity of the restriction endonuclease *Eco*RI. (A) Agarose gel electrophoresis of pBR322 DNA following the action of restriction endonuclease *Eco*RI for various lengths of time. Reaction media and procedures were as indicated under Materials and Methods. Samples were withdrawn at the indicated time from the reaction medium and subjected to electrophoresis. (A1) Control experiments performed in the absence of drug. (A2) Experiments performed in the presence of 10^{-8} M Net–OPC. (B) Steady-state profile of form II DNA concentration (open circle resulting from the occurrence of a single-strand break). Lines were the best fits to data points of the exponential association (eq 11) describing the variation of the form II concentration as a function of time obtained in the absence of drug (solid line), in the presence of 10^{-8} M Net–OPC (dashed line), and in the presence of 10^{-7} M Net–OPC (dotted line).

1988). Under these circumstances, the steady-state profile of the variation of the DNA form II concentration as a function of time is described by the exponential association equation

$$[\mathrm{FII}] = A\,[1 - \exp(-klt)] + C[1 - \exp(-k2t)] + E \quad (11)$$

where E depends on the amount of form II initially present before the action of the enzyme. Values of A, k_1, k_2, and C have been estimated from the goodness-of-fit assessed by using actual distances provided by a Marquardt procedure. Figure 8B shows a typical example of such treatment, in which is represented the evolution of the concentration of DNA form II as a function of time in the absence and in the presence of Net–OPC. The r^2 value close to 1 as well as the estimated percent error clearly show that the experimental values account for eq 10 both in the presence and in the absence of drug. This treatment leads to the estimation of the rate constant k_2 of the second strand break, which appears to be the limiting factor of the overall enzymatic reaction. This is in agreement with the occurrence of a two-step consecutive reaction with an obligatory intermediate. Under these operating conditions, k_1 and k_2 yielded average values of 0.50 ± 0.05 min^{-1} and 0.34 ± 0.01 min^{-1} for *Eco*RI and 0.21 min^{-1} and 0.20 min^{-1} in the case of *Nru*I. We have estimated the inhibition of the catalytic activity of the enzymes from the decrease of the rate constants k_1 and k_2 observed in the presence of increasing concentrations of drug. Efficiency of the inhibition is provided by the EC_{50} value, which corresponds to the concentration of drug that decreases by 50% the rate constant. Values summarized in Table III show that, compared to netropsin, Net–OPC displays a more pronounced inhibitory effect on *Eco*RI activity, affecting both k_1 and k_2. The selective inhibition of Net–OPC on *Eco*RI is obvious from the lack of effect of the drug on *Nru*I activity at concentrations up to 50 μM. Moreover, it is of interest to notice that the selective action (effect on *Eco*RI versus effect on *Nru*I) is markedly higher with Net–OPC than with netropsin. Finally, the addition of OPC alone up to 50 μM in the assay medium did not result in any significant inhibition of *Eco*RI activity.

Table III: Effects of Netropsin, Net–OPC, and OPC on the Catalytic Activity of the Restriction Endonucleases *Eco*RI and *Nru*I[a]

	*Eco*RI		*Nru*I	
	k_1	k_2	k_1	k_2
netropsin	1.3	0.85	26	29
Net–OPC	0.01	0.02	>50	>50
OPC	>50	>50		
pentyl-OPC	>50	>50		

[a] Enzymatic activities were measured as described under Materials and Methods and are illustrated in Figure 8. k_1 and k_2 are the pseudo-first-order rate constants of the first and the second DNA strand break produced by the enzymes. Values indicated are the concentration of drug (micromolar) that reduced by 50% (EC_{50}) the corresponding rate constants.

Discussion

Binding to DNA and Polynucleotides. In order to develop sequence-specific DNA-binding molecules for pharmacological purposes, we have synthesized a hybrid groove-binder–intercalator composed of a netropsin moiety covalently linked to the intercalating chromophore oxazolopyridocarbazole (OPC). First of all, the question arises as to whether the presence of the intercalating agent instead of a guanidine residue markedly modifies the properties of the netropsin moiety in terms of A-T preference and sequence recognition. As does the parent compound netropsin, the hybrid molecule Net–OPC preferentially binds to A-T-rich double-stranded polynucleotide. The fluorescence increase of the OPC chromophore upon binding clearly indicates that the OPC moiety is involved in the binding process. A Scatchard plot of the binding curves indicates that, in poly[d(A-T)], Net–OPC binds to at least two different binding sites with K_{app} values close to 6.0×10^8 and 7.0×10^6 M^{-1} in the presence of 100 mM NaCl, whereas in poly[d(G-C)], the molecule binds to a single type of binding site with K_{app} close to 2.0×10^6 M^{-1}. The occurrence of at least two individual types of binding sites in poly[d(A-T)] is confirmed by the broadening of the melting curve of poly[d(A-T)] and the decrease of the cooperative index of the melting process observed at saturating concentration of drug. These features could be the consequence of the occurrence of a heterogeneous stabilization of the DNA duplex upon drug binding, resulting in turn from the heterogeneous nature of the binding. Accordingly, the involvement of two or one positive charges in the binding to the sites of higher and lower affinity, respectively, indicates that the mode of binding of Net–OPC to these sites is different. The slope value (1.0) of the straight line that

expresses the viscosity of sonicated A-T-rich DNA as a function of the amount of Net–OPC bound suggests that the OPC chromophore is distributed in both intercalating and external binding sites since, under similar experimental conditions, the binding of OPC alone yields a slope value of 2.1. The low value of energy transfer from A-T bases to bound OPC is also in agreement with a heterogeneous distribution of the OPC chromophore in intercalating and external binding sites. Considering the size of the high-affinity binding site (about 8 bp), it seems reasonable to suggest that the OPC chromophore is not intercalated and that both moieties of Net–OPC are bound to DNA only inside the minor groove. In this circumstance, the binding to the site of lower affinity should preferentially occur according to an intercalating mode. However, the involvement of one positive charge only in the binding to this site suggests that the bis(pyrrole) moiety of the drug should remain outside of the double helix. These observations suggest that intercalation of the OPC chromophore and selective binding of the netropsin moiety to A-T base pairs cannot take place simultaneously. In poly[d(G-C)], the mode of binding appears to be markedly different, since the major part of the population of Net–OPC molecules that are bound to the single site appears to be intercalated. The apparent binding site size of about 2 base pairs provided by the Scatchard plot is also in agreement with intercalation. It is possible that in G-C base pairs, because of the steric hindrance of the amine of guanine, the bis(pyrrole) chain could bind at the external part of the groove, allowing the intercalation of OPC.

Sequence Recognition. In view of sequence selective recognition, footprinting experiments clearly show that, at low concentration, Net–OPC efficiently protects the TTA-containing sequence at the *Eco*RI site against $OH^{\bullet}$ radical mediated degradation. Additional sequences significantly protected are CTT at positions close to the *Eco*RI site, TT and CT. It is of interest to notice that, in this DNA fragment, all protected regions contain CTT or CT base pairs. It should be noticed as well that Harshman and Dervan (1985) have detected strong protection in the presence of netropsin at sequences containing a CTT run. The region of the *Eco*RI site displays in fact two 3′ → 5′ CTT runs and one 5′ → 3′ TTCTT run.

Effects on Restriction Endonucleases. The selective binding of Net–OPC to the *Eco*RI site is markedly well confirmed by the selective inhibitory effect of the drug on the catalytic activity of the endonuclease *Eco*RI. The inhibitory effect on the first break promoted by the enzyme appears to be 100 times more efficient than that observed in the presence of netropsin. The striking observation is the absence of inhibitory effect on the activity of the enzyme *Nru*I, which strongly suggests that the inhibition of *Eco*RI by Net–OPC is in direct relation with the sequence recognition. In contrast, netropsin appears to be less selective than Net–OPC, since significant inhibition of *Nru*I can be observed at lower concentrations in the range of 20 μM. Similarily, it has previously been suggested that the inhibitory effects of netropsin and distamycin on the *Eco*RI activity were not related to sequence recognition (Goppelt et al., 1981).

Conclusion. The linkage of the intercalating chromophore OPC to a bis(pyrrolecarboxamide) moiety related to netropsin resulted in a hybrid groove-binder–intercalator displaying the following main properties: (i) As does the parent compound netropsin, the hybrid preferentially binds to A-T-containing nucleotides. (ii) In poly[d(A-T)], the binding occurs at two different binding sites involving either the intercalation or the external binding of the chromophore. The binding constant to the high-affinity site estimated from the melting experiments is markedly higher than that displayed by netropsin. (iii) Hydroxyl radical footprinting shows that Net–OPC fully protects the *Eco*RI site and recognizes as well the CTT sequence. The protection of the *Eco*RI site results in a strong and selective inhibition of the enzyme occurring to a higher extent than that produced by netropsin.

Acknowledgments

We gratefully thank Monique Quesne and Eliane Franque for skilled technical assistance as well as Dr. A. K. Larsen for help in editing the manuscript.

Registry No. Net-OPC, 130861-48-2; poly[d(A-T)], 26966-61-0; poly[d(G-C)], 62081-33-8.

References

Auclair, C., & Paoletti, C. (1981) *J. Med. Chem. 24*, 289.
Auclair, C., Voisin, E., Banoun, H., Paoletti, C., Bernadou, J., & Meunier, B. (1984) *J. Med. Chem. 27*, 1161.
Auclair, C., Schwaller, M. A., Renê, B., Banoun, H., Saucier, J. M., & Larsen, A. K. (1988) *Anti-Cancer Drug Des. 3*, 133.
Crothers, D. M. (1971) *Biopolymers 10*, 2147.
Dervan, P. B. (1986) *Science 232*, 464.
Dryer, G. B., & Dervan, P. B. (1985) *Proc. Natl. Acad. Sci. U.S.A. 82*, 968.
Goppelt, M., Langowski, J., Pingoud, A., Haupt, W., Urbank, C., Mayer, H., & Maass, G. (1981) *Nucleic Acids Res. 9*, 6115.
Gouyette, A., Auclair, C., & Paoletti, C. (1985) *Biochem. Biophys. Res. Commun. 131*, 614.
Green, P. J., Pines, O., & Inouye, M. (1986) *Annu. Rev. Biochem. 55*, 569.
Halford, S. E., & Goodall, A. J. (1988) *Biochemistry 27*, 1771.
Harshman, K. D., & Dervan, P. B. (1985) *Nucleic Acids Res. 13*, 4825.
Izant, J. G., & Weintraub, H. (1984) *Cell 36*, 1007.
Izant, J. G., & Weintraub, H. (1985) *Science 229*, 345.
Kansal, V. K., Sundaramoorthi, R., Das, B. C., & Potier, P. (1985) *Tetrahedron Lett. 40*, 4933.
Kopka, M. L., Yoon, C., Goodsell, D., Pjura, P., & Dickerson, R. E. (1985a) *Proc. Natl. Acad. Sci. U.S.A. 82*, 1376.
Kopka, M. L., Yoon, C., Goodsell, D., Pjura, P., & Dickerson, R. E. (1985b) *J. Mol. Biol. 183*, 553.
Larsen, A. K., Paoletti, J., Belehradek, J. R., & Paoletti, C. (1986) *Cancer Res. 46*, 5236.
Le Pecq, J. B., & Paoletti, C. (1967) *J. Mol. Biol. 27*, 87.
Lown, J. W. (1988) *Anti-Cancer Drug Des. 3*, 25.
Lown, J. W., & Krowicki, K. (1985) *J. Org. Chem. 50*, 3774.
Marky, L. A., & Breslauer, K. J. (1982) *Biopolymers 21*, 2185.
Morvan, F., Rayner, B., Imbach, J. L., Chang, D. K., & Lown, J. W. (1987) *Nucleic Acids Res. 15*, 4241.
Mrani, D., Gosselin, G., Auclair, C., Balzarini, J., De Clercq, E., Paoletti, C., & Irbach, J. L. (1991) *Eur. J. Med. Chem.* (in press).
Paoletti, C. (1988) *Anti-Cancer Drug Des. 2*, 325.
Record, M. T., Lohman, T. M., & De Haseth, P. L. (1976) *J. Mol. Biol. 107*, 145.
Reinhardt, C. G., Roques, B. P., & Le Pecq, J. B. (1982) *Biochem. Biophys. Res. Commun. 4*, 1376.
Saucier, J. M., Festy, B., & Le Pecq, J. B. (1971) *Biochimie 53*, 973.
Scatchard, G. (1949) *Ann. N.Y. Acad. Sci. 51*, 660.

Schultz, P. G., Taylor, J. S., & Dervan, P. B. (1982) *J. Am. Chem. Soc. 104*, 6861.
Sequin, U. (1974) *Helv. Chim. Acta 57*, 68.
Taylor, J. S., Schultz, P. G., & Dervan, P. B. (1984) *Tetrahedron 40*, 457.
Toulmé, J. J., Krish, H. M., Loreau, N., Thuong, N. T., & Hélene, C. (1986) *Proc. Natl. Acad. Sci. U.S.A. 83*, 1927.
Weil, G., & Calvin, M. (1963) *Biopolymers 1*, 401.
Zimmer, C., & Wähnert, U. (1986) *Prog. Biophys. Mol. Biol. 47*, 31.

Comparative Circular Dichroism and Fluorescence Studies of Oligodeoxyribonucleotide and Oligodeoxyribonucleoside Methylphosphonate Pyrimidine Strands in Duplex and Triplex Formation†

Daniel E. Callahan, Tina L. Trapane, Paul S. Miller, Paul O. P. Ts'o, and Lou-Sing Kan*

Department of Biochemistry, School of Hygiene and Public Health, The Johns Hopkins University, 615 North Wolfe Street, Baltimore, Maryland 21205

Received June 20, 1990; Revised Manuscript Received October 29, 1990

ABSTRACT: An analogue of the homopyrimidine oligodeoxyribonucleotide $d(CT)_8$ has been synthesized. This analogue, $d(\underline{CT})_8$ contains nonionic methylphosphonate internucleoside linkages. The pH-dependent conformational transitions of $d(\underline{CT})_8$ have been studied and its ability to form duplexes and triplexes with the normal homopurine oligonucleotide $d(AG)_8$ has also been investigated as a function of pH. Circular dichroism spectroscopy and ethidium bromide fluorescence enhancement have been used to monitor pH-dependent conformational transitions driven by the protonation of cytosine residues, and the different behavior of $d(\underline{CT})_8$ and $d(CT)_8$ has been compared. It was possible to form self-associated complexes by using either $d(CT)_8$ or $d(\underline{CT})_8$, and both compounds combined with $d(AG)_8$ to form duplex or triplex DNA. At neutral pH, the CD spectrum of $d(AG)_8{\cdot}d(\underline{CT})_8$ duplex was quite different from the CD spectrum of $d(AG)_8{\cdot}d(CT)_8$ duplex, reflecting most likely a difference in conformation. The duplex to triplex transition characteristic of this DNA sequence occurred at a lower pH when $d(\underline{CT})_8$ was substituted for $d(CT)_8$; however, at pH 4.2, triplex containing $d(\underline{CT})_8$ was similar in conformation to triplex containing $d(CT)_8$. Several of these observations can be related to the alterations in electrostatic and steric interactions that occur when the negatively charged phosphodiester backbone of $d(CT)_8$ is replaced with a nonionic methylphosphonate backbone.

Oligodeoxyribonucleoside methylphosphonates are nucleic acid analogues containing nonionic methylphosphonate internucleoside linkages in place of the naturally occurring, negatively charged phosphodiester linkages (Miller & Ts'o, 1987). Methylphosphonates are nuclease-resistant and are taken up readily by mammalian cells in culture (Miller et al., 1981). One goal in the development of such compounds is the regulation of gene expression in living cells. Methylphosphonates can regulate gene expression at the level of mRNA translation by binding to complementary mRNA or precursor mRNA targets (Agris et al., 1986; Kean et al., 1988; Yu et al., 1989; Kulka et al., 1989). In such cases, duplex formation between the methylphosphonate and the mRNA target prevents the translation or processing of a particular mRNA transcript. Another goal in the development of these compounds is the regulation of gene expression at the transcriptional level by sequence-specific triplex formation with DNA. As has been recently described, the target in this case is a double-stranded, duplex DNA rather than single-stranded mRNA (Maher et al., 1989). The presence of a third strand in the major groove of a DNA duplex could hinder the binding of proteins or enzymes and thus prevent the production of a particular mRNA transcript.

Methylphosphonate-substituted oligodeoxyribonucleotides can bind to single-stranded DNA, and the resultant hybrid duplexes (containing one phosphodiester strand and one methylphosphonate strand) have altered stability relative to phosphodiester duplexes (Quartin & Wetmur, 1989). The changes in stability are dependent upon ionic strength and are due in part to the alteration of electrostatic interactions that occur when negatively charged phosphodiester linkages are replaced with nonionic methylphosphonate linkages. A steric factor is also partially responsible for the altered stability of these hybrid duplexes. During synthesis of these compounds, one of the two stereoisomers (either R_p or S_p configuration) is formed at each methylphosphonate linkage (Miller et al., 1979); thus, preparations of fully substituted methylphosphonate oligomers are a mixture of diastereomers, making it difficult to assess the contribution of the steric factor to duplex stability. The studies presented here empirically assess the effect of methylphosphonate substitution on the conformation of a hybrid duplex or triplex of deoxyoligonucleotides.

†This work was supported in part by DOE (Grant DE-FG02-88ER60636) and by NCI (Grant 5 PO1 CA42762-03). Preliminary results have been presented at the 34th annual meeting of the Biophysical Society, Baltimore, MD, February 1990.

*To whom correspondence should be addressed.

0006-2960/91/0430-1650$02.50/0